



Pergamon

SCIENCE @ DIRECT®

Bioorganic & Medicinal Chemistry Letters 13 (2003) 3161–3166

BIOORGANIC &
MEDICINAL
CHEMISTRY
LETTERS

Reversed Hydroxamate-Bearing Thermolysin Inhibitors Mimic a High-Energy Intermediate Along the Enzyme-Catalyzed Proteolytic Reaction Pathway

Jung Dae Park and Dong H. Kim*

Center for Integrated Molecular Systems, Division of Molecular and Life Sciences,
Pohang University of Science and Technology, San 31 Hyojadong, Pohang 790-784, South Korea

Received 12 May 2003; accepted 4 July 2003

Abstract—A series of inhibitors that bear a reversed hydroxamate moiety have been evaluated as transition state analogue inhibitors for thermolysin. A linear correlation is observed between the K_i values of these inhibitors and the kinetic parameters (K_M/k_{cat}) of the parallel series of related substrates, satisfying the criterion stipulated for transition state analogue inhibitors by Bartlett and Marlowe. Furthermore, examination of the binding mode of a related reversed hydroxamate bearing thermolysin inhibitor, in comparison with a transition state postulated for the enzyme-catalyzed proteolytic reaction revealed that the inhibitors under study mimic the electronic as well as the geometric characteristics of the transition state. On the basis of these results it may be concluded that the hydroxamate-bearing zinc protease inhibitors are a new type of transition state analogue inhibitors.

© 2003 Elsevier Ltd. All rights reserved.

Zinc proteases constitute one of largest families of proteolytic enzymes.¹ These enzymes carry a catalytically essential zinc ion at their active site. Thermolysin (TLN, EC 3.4.24.4) isolated from *Bacillus thermoproteolyticus* is one of most extensively studied zinc proteases. Thermolysin cleaves the amino side peptide bond of the amino acid residue having a hydrophobic side chain.² The enzyme has been used as a model target enzyme for developing inhibitor design strategies that can be transferred to zinc proteases of medicinal interests, such as angiotensin converting enzyme³ and matrix metalloproteases.⁴ Most of small molecule inhibitors for the zinc proteases are designed by incorporating a zinc ligating group into a molecular scaffold that resembles substrate so that it can be recognized by the enzyme and forms a complex with it.⁵ Carboxylate, thiol and hydroxamate are commonly used for such zinc-coordinating group. Of these zinc ligating groups, hydroxamate occupies a prominent position because of its strong chelating property toward zinc ion. Another widely employed design strategy involves construction of a small molecule whose structure can mimic a transition state in the enzyme catalyzed reaction, and this approach has its

theoretical basis on the transition state theory proposed for enzymic catalytic reactions.⁶ According to the theory, enzyme lowers the activation energy in the enzymic reaction by stabilizing a transition state along the reaction path through stronger interactions relative to the ground state of substrate.⁶ It is, therefore, expected that chemically stable analogues of the transition state would bind the enzyme more strongly than substrate and thus inhibit the enzymic activity.⁷

Although the theoretical background for transition state analogue inhibition is well founded, the transition state analogue inhibitors has not been rigorously defined and the terminology is used as a conceptual descriptor. Thus, inhibitors are ordinarily classified as transition state analogue inhibitors if they are designed in such a way that they bear, in place of the scissile peptide bond, a moiety that resembles structurally a postulated transition state in the enzymic reaction and exhibit such kinetic features as a very low K_i value and slow inhibition rate. Recently, Bartlett and Marlowe⁸ have proposed a criterion for testing transition state analogue inhibitors: According to them, there exists a linear correlation between K_i values for a series of transition state analogue inhibitors and K_M/k_{cat} values for a parallel series of the corresponding substrates, as represented by eq 1:

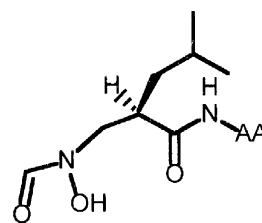
*Corresponding author: Tel.: +82-54-279-2101; fax: +82-54-279-5877; e-mail: dhkim@postech.ac.kr

$$\log K_i = \log (K_m/k_{\text{cat}}) + \log dk_{\text{uncat}} \quad (1)$$

Thus, for transition state analogue inhibitors, there is obtained a straight line with a slope = 1 when $\log K_i$ values of a series of the transition state analogue inhibitors are plotted against $\log K_m/k_{\text{cat}}$ value for a series of the corresponding substrates whose structures are altered in such a way that the alteration does not affect the rate of the noncatalyzed reaction.^{8,9} The criterion has been successfully applied for assessing phosphorous-containing substrate analogues as transition state analogue inhibitors for TLN^{8,9} and carboxypeptidase A.¹⁰

Recently, we have reported that *N*-formyl-*N*-hydroxy- β -phenylalanine *N*-methylamide (HCONOH - β - Phe - NHMe) is a potent competitive TLN inhibitor having the K_i value of $1.66 \pm 0.05 \mu\text{M}$.¹¹ It was thought to be of interest to evaluate the reversed hydroxamate-bearing TLN inhibitors as transition state analogue inhibitors and we undertook the present study to find that inhibitors of this type fulfill the criterion set forth by Bartlett and Marlowe for transition state analogue inhibitors.

We chose to use the same series of tripeptide substrates as those used by Bartlett and Marlowe⁸ for their study for assessing phosphonamidates as transition state mimics in the TLN-catalyzed proteolysis. These substrates bear a L-Leu residue in common at the P_1' site and varied P_2' residues. We have then synthesized a series of hydroxamate-bearing inhibitors (**1a–e**), which bear a L-Leu residue at the P_1' site and the same series of residues as those in the substrates at the P_2' site.



1a : AA = H

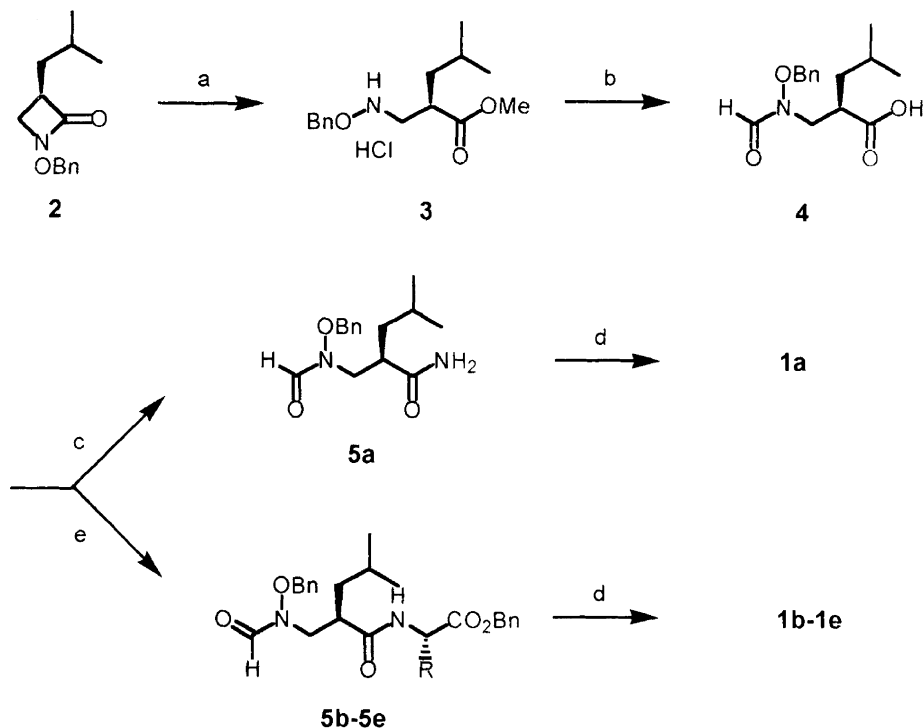
1b : AA = Gly

1c : AA = L-Ala

1d : AA = D-Ala

1e : AA = L-Phe

The synthetic route for the preparation of the inhibitors is outlined in Scheme 1. (3*R*)-*N*-Benzyloxy-3-isobutyl-2-azetidine (**2**) that was prepared from 4-methylvaleric acid in eight steps according to the method reported by Jin and Kim¹¹ was treated with methanol in the presence of trimethylsilyl chloride to give **3**. *N*-Formylation of the latter with sodium formate and acetic anhydride in anhydrous formic acid gave **4**. Treatment of **4** with concentrated ammonium hydroxide in the presence of isobutylchloroformate and *N*-methylmorpholine gave **5a** which was converted into **1a** by hydrogenolysis. Similarly, treatment of **4** with an appropriate amino acid in the form of a benzyl ester afforded **5b–e**, which were then subjected to hydrogenolysis to obtain **1b–e**.¹²



Scheme 1. Reagents, conditions, and yield: (a) chlorotrimethylsilane (4 equiv), MeOH, rt, 2 h, 92%; (b) (i) 3 N HCl, reflux, 2 h; (ii) NaCO₂H (1.2 equiv), Ac₂O (3 equiv), HCO₂H, rt, 12 h, 83%; (c) isobutylchloroformate, 4-methylmorpholine, NH₄OH, rt, 6 h, 56%; (d) H₂, Pd/C, MeOH, rt, 2 h, 88–95%; (e) isobutylchloroformate, 4-methylmorpholine, the desired amino acid benzyl ester, rt, 2 h, 65–78%.

The compounds synthesized were assayed for TLN inhibition. Inhibition constants (K_i values) were determined using *N*-[3-(2-furyl)acryloyl]-Gly-L-leucineamide (FA-Gly-L-Leu-NH₂) as substrate at pH 7.2 as described in the literature¹³ and are collected in Table 1. Inhibitor **1e** having Phe at the C-terminal binds TLN most tightly with the K_i value of 1.84 μ M. Inhibition constants for **1a** and **1d** are decreased by 29- and 208-fold, respectively, compared with that of **1e**, suggesting that the amino acid residue at the P₂' plays an important role in binding of the inhibitors to TLN. Comparison of the K_i values of the series of inhibitors with the K_m values of substrates in a parallel series is made graphically (Fig. 1). As can be seen in Figure 1, no correlation is found between K_i values for the inhibitors and the K_m values of the corresponding substrates, indicating that the inhibitors are not ground state analogues. However, plotting of $\log K_i$ versus $\log K_m/k_{cat}$ according to eq 1 gives a straight line (Fig. 2), whose linear regression yields a slope of 0.99 ($R=0.98$), which suggests strongly that the reversed hydroxamate moiety in the inhibitors may mimic a transition state or a high-energy intermediate generated by the attack of a water molecule to the scissile peptide bond of substrate in the enzymatic proteolysis reaction pathway.

An additional evidence for support that hydroxamate may mimic a transition state in the TLN-catalyzed proteolytic reaction has been obtained by comparing the binding mode of a hydroxamate-bearing inhibitor to TLN with a postulated transition state in the enzymic reaction. Mechanism of TLN-catalyzed proteolytic reaction has been the subject of intensive investigations.

Table 1. Kinetic constants for inhibition of thermolysin and thermolysin-catalyzed proteolysis

Inhibitor	K_i (μ M)	Corresponding substrate ^a	
		K_i (μ M)	K_m/k_{cat} (μ M/s)
1d	383	16.6	3200
1a	52.8	20.6	196
1b	14.7	10.87	165
1e	1.84	2.4	20
1c	2.49	10.6	13.6

^aFrom ref 21.

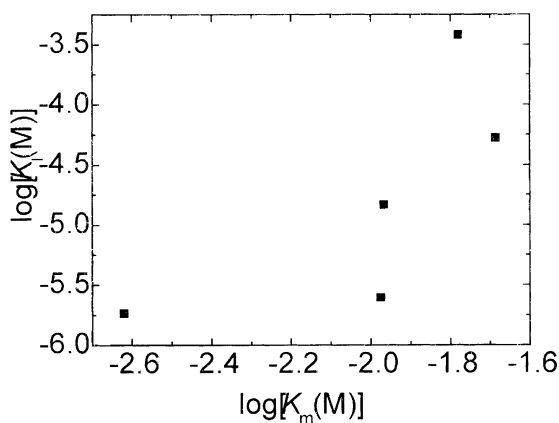


Figure 1.

A variety of tools and methods such as X-ray crystallographic studies,¹⁴ kinetic investigations,¹⁵ site directed mutagenesis,¹⁶ interactive computer graphics,¹⁷ and quantum chemical calculations¹⁸ have been employed in the investigations, and numerous reaction pathways, although differ each other only in minor detail, have been proposed. All these proposed mechanisms postulate in common a tetrahedral *gem*-diolate transition state that is generated by the nucleophilic attack of the zinc-bound activated water molecule on the carbonyl carbon of the scissile peptide bond. The carbonyl oxygen of the scissile bond is formally uncharged in the ground state, but acquires a negative charge as the reaction proceeds, and the transition state is stabilized via coordination with the active site zinc ion and through hydrogen bonding with the imidazole of His-231 as depicted schematically in Figure 3. The binding mode of HCONOH- β -Phe-NHMe to TLN has been revealed by the X-ray diffraction analysis of the complex of TLN with the inhibitor.¹⁹ Figure 4 is a schematic representation of the binding mode of HCONOH- β -Phe-NHMe to TLN. It can be seen in Figure 4 that the two oxygen atoms of the hydroxamate moiety bind the zinc ion in a bidentate fashion with distances of 2.00 and 2.36 Å and the protonated carboxylate of Glu-143 is engaged in a hydrogen bonding with the carbonyl oxygen of the inhibitor. The distance of 2.00 Å for the bond between the *N*-hydroxyl oxygen and the zinc ion is worthy of noting and suggests that the hydroxyl oxygen

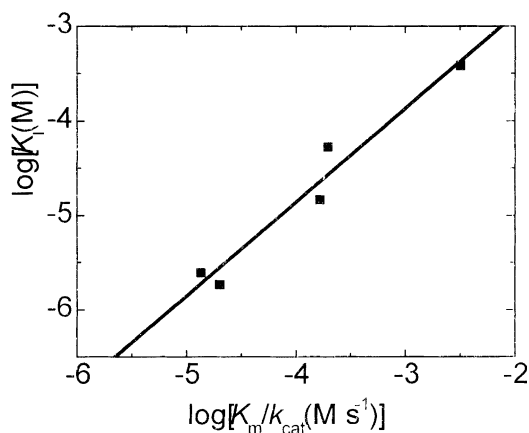


Figure 2.

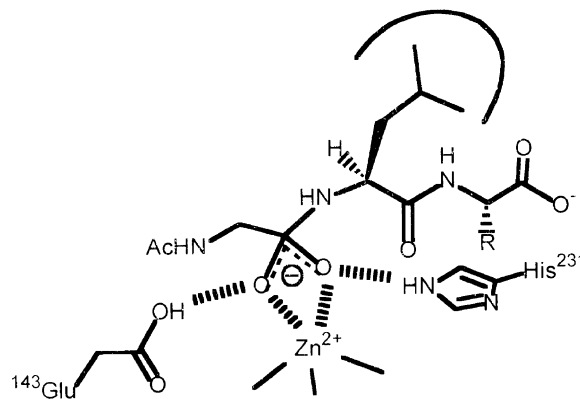


Figure 3.

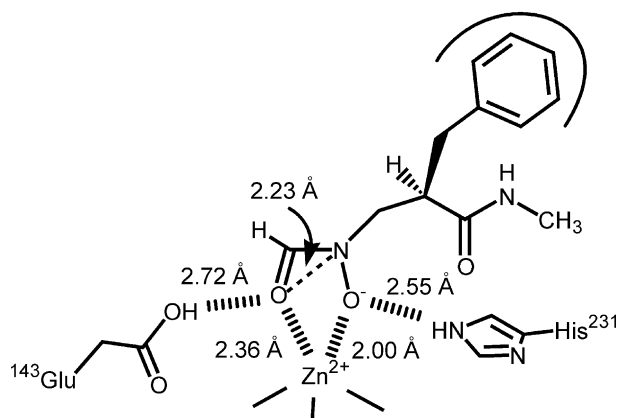


Figure 4.

binds the zinc ion in a deprotonated form in reminiscence of the postulated diolate transition state.²⁰ The deprotonated hydroxyl oxygen of the hydroxamate is hydrogen bonded to a nitrogen of the imidazole moiety in His-231. The tetrahedrality of the zinc-bound hydroxamate moiety may be visualized by envisioning an imaginary bond between the hydroxamate nitrogen and the formyl oxygen, the distance of which is estimated to be 2.23 Å. This distance is considerably longer than a normal C–O bond but can be reconciled with the proposition that the hydroxamate may represent an early stage of the postulated transition state. It may be thus inferred from the foregoing comparison that the reversed hydroxamate moiety mimics the electronic as well as the geometric characteristics of the transition state in the enzyme catalyzed proteolytic reaction.

Conclusion

The linear correlation observed between K_i values and K_m/k_{cat} for inhibitors **1a–e** and the corresponding substrates coupled with the binding feature of the reversed hydroxamate in forming the TLN·HCONOH-β-Phe-NHMe complex suggest strongly that compounds **1a–e** are a novel type of transition state analogue inhibitors for TLN, and a hydroxamate moiety would mimic a diolate transition state postulated for the TLN-catalyzed proteolytic reaction pathway. The results of the present study imply that many of reversed hydroxamate as well as hydroxamate type inhibitors developed for zinc proteases including MMPs may function as transition state analogue inhibitors.

Acknowledgements

The work was supported by Korea Research Foundation Grant (KRF-2000-015-DS0025).

References and Notes

1. Lipscomb, N. W.; Sträter, N. *Chem. Rev.* **1996**, *96*, 2375.
2. Beynon, R. J.; Beaumont, A. In *Handbook of Proteolytic Enzymes*; Barrett, A. J., Rawlings, N. D., Woessner, J. F. Eds.; Academic: New York, 1998; p 1037.

3. Zuman, M. A.; Oparil, S.; Calhoun, D. A. *Nat. Rev. Drug Discov.* **2002**, *1*, 621.
4. Wittaker, M.; Floyd, D. D.; Brown, P.; Gearing, A. J. H. *Chem. Rev.* **1999**, *99*, 2735.
5. Powers, J. C.; Harper, J. W. Inhibitors of Metalloproteases. In *Protease Inhibitors*; Barrett, A. J., Salvesen, G., Eds.; Elsevier Science: Amsterdam, 1986; p 219.
6. (a) Kraut, J. *Science* **1988**, *242*, 533. (b) Cannon, W. R.; Sergleton, S. F.; Benkovic, S. J. *Nat. Struct. Biol.* **1996**, *3*, 821.
7. (a) Wolfenden, R. *Acc. Chem. Res.* **1972**, *5*, 10. (b) Lienhard, G. E. *Science* **1973**, *180*, 149. (c) Wolfenden, R. Transition State Affinity and the Design of Enzyme Inhibitors. In *Enzyme Mechanisms*; Page, M. I., Williams, A., Eds.; Royal Chemical Society: London, 1987; p 97.
8. Bartlett, P. A.; Marlowe, C. K. *Biochemistry* **1983**, *22*, 4618.
9. Mader, M. M.; Bartlett, P. A. *Chem. Rev.* **1997**, *97*, 1281.
10. Hanson, J. E.; Kaplan, A. P.; Bartlett, P. A. *Biochemistry* **1989**, *28*, 6294.
11. Jin, Y.; Kim, D. H. *Bioorg. Med. Chem. Lett.* **1998**, *8*, 3515.
12. (R)-2-(N-(O-Benzoyloxy)aminomethyl)-4-methylpentanoic acid methyl ester hydrochloride (**3**). To the solution of **2** (9.0 g, 38.6 mmol) in anhydrous MeOH (100 mL) was added slowly chlorotrimethylsilane (19.6 mL, 0.154 mol) under nitrogen atmosphere. The resulting solution was stirred for 2 h and evaporated under reduced pressure to afford a white solid, which was recrystallized from methanol and ether to give a white crystal (10.7 g, 92%). Mp 116.5–117°C; $[\alpha]_D^{20} + 6.5^\circ$ (c 0.65, DMSO); IR (KBr) 1738 cm^{-1} ; ^1H NMR (DMSO- d_6 , 300 MHz) δ 0.83 (q, 6H), 1.31–1.48 (m, 3H), 2.88 (m, 1H), 3.14–3.34 (m, 2H), 4.95 (s, 2H), 7.32–7.39 (m, 5H); ^{13}C NMR (DMSO- d_6 , 300 MHz) δ 22.6, 23.5, 26.2, 40.0, 51.2, 52.5, 75.6, 129.4, 129.7, 129.8, 135.1, 174.9.
- (R)-2-((N-(O-Benzoyloxy)-N-formyl)aminomethyl)-4-methylpentanoic acid (**4**). A mixture of **3** (10.0 g, 33.1 mmol) and 3 N HCl (100 mL) was refluxed for 2 h, then evaporated under reduced pressure to give (R)-2-(N-(O-benzoyloxy)-aminomethyl)-4-methylpentanoic acid hydrochloride as a white powder (quantitative). To an ice-chilled solution of sodium formate (2.7 g, 39.8 mmol) and (R)-2-(N-(O-benzoyloxy)-aminomethyl)-4-methylpentanoic acid hydrochloride in anhydrous formic acid (50 mL) was added slowly acetic anhydride (9.4 mL, 99.4 mmol) and the resulting solution was stirred for 12 h at room temperature. The reaction mixture was evaporated under reduced pressure. The residue was dissolved in ethyl acetate (100 mL), washed successively with 1 N HCl solution (50 mL×3) and brine (50 mL×3), and dried over anhydrous MgSO_4 . The crude product was purified by column chromatography (EtOAc/n-hexane = 1/2) to give the product as a pale yellow oil (7.68 g, 83%); $[\alpha]_D^{25} + 2.6^\circ$ (c 0.5, MeOH); IR (CHCl_3) 1669, 1731 cm^{-1} ; ^1H NMR (CDCl_3 , 300 MHz) δ 0.89 (d, 6H), 1.24 (m, 1H), 1.59 (m, 2H), 2.04 (d, 1H), 2.82 (m, 1H), 3.85 (m, 1H), 4.81 (s, 2H), 7.35 (m, 5H), 7.97 (s, 3/10H), 8.12 (s, 7/10H); ^{13}C NMR (CDCl_3 , 300 MHz) δ 14.6, 20.7, 22.4, 23.3, 26.2, 39.2, 42.3, 46.0, 129.1, 129.4, 129.8, 134.5, 163.2, 180.4. HRMS (FAB+) (M+H)⁺: calcd for $\text{C}_{15}\text{H}_{22}\text{NO}_4$, 280.1549; found 280.1546.
- (R)-2-((N-(O-Benzoyloxy)-N-formyl)aminomethyl)-4-methylpentanoic acid amide (**5a**). To an ice-chilled solution of **4** (0.35 g, 1.25 mmol) in anhydrous THF was added isobutylchloroformate (0.18 mL, 1.25 mmol) and NMO (0.14 mL, 1.25 mmol) and the resulting mixture was stirred for 15 min at 0°C. To the reaction mixture was added concd NH_4OH solution (0.6 mL, 5 mmol) and then stirred for 6 h at room temperature. The reaction mixture was evaporated under reduced pressure. The residue was dissolved in ethyl acetate (20 mL), washed successively with 1 N HCl solution (20 mL×3), 5% NaHCO_3 solution (20 mL×3), and brine (20 mL×3), and

dried over anhydrous MgSO_4 . The crude product was purified by column chromatography ($\text{EtOAc}/n\text{-hexane}=1/1$) to give the product as an oil (0.20 g, 56%). $[\alpha]_{\text{D}}^{25} +1.0^\circ$ (c 1.0, CHCl_3); IR (CHCl_3) 1666, 1685 cm^{-1} ; ^1H NMR (CDCl_3 , 300 MHz) δ 0.88 (d, 6H), 1.26 (m, 1H), 1.59 (m, 2H), 2.67 (m, 1H), 3.69 (m, 2H), 4.84 (s, 2H), 5.55–5.74 (m, 2H), 7.24–7.38 (m, 5H), 7.82 (s, 3/10H), 8.21 (s, 7/10H); ^{13}C NMR (CDCl_3 , 300 MHz) δ 22.5, 23.4, 26.2, 40.0, 43.0, 62.4, 129.1, 129.6, 129.9, 134.5, 163.9, 176.6, 205.3. HRMS (FAB+) ($\text{M}+\text{H}^+$): calcd for $\text{C}_{15}\text{H}_{23}\text{N}_2\text{O}_3$, 279.1709; found 279.1708.

General procedure for the preparation of 5b–5e. To an ice-chilled solution of **4** in anhydrous CH_2Cl_2 was added isobutylchloroformate (1 equiv) and NMO (2 equiv) and the resulting mixture was stirred for 15 min at 0°C . To the reaction mixture was added the solution of the corresponding amino acid benzyl ester (1 equiv) and then stirred for 2–4 h at room temperature. The reaction mixture was evaporated under reduced pressure. The residue was dissolved in ethyl acetate (50 mL), washed successively with 1N HCl solution (50 mL \times 3), 5% NaHCO_3 solution (50 mL \times 3), and brine (50 mL \times 3), and dried over anhydrous MgSO_4 . The crude product was purified by column chromatography ($\text{EtOAc}/n\text{-hexane}=1/2$) to give the product as an oil.

***N*-[(*R*)-2-((*N*-(*O*-Benzyloxy)-*N*-formyl)aminomethyl)-4-methylpentanoyl]glycine benzyl ester (5b).** (Yield, 65%). $[\alpha]_{\text{D}}^{20} -13.1^\circ$ (c 2.04, CHCl_3); IR (CHCl_3) 1653, 1684, 1750 cm^{-1} ; ^1H NMR (CDCl_3 , 300 MHz) δ 0.87 (d, 6H), 1.07–1.25 (m, 1H), 1.59 (m, 2H), 2.67 (m, 1H), 3.06–3.73 (m, 2H), 3.894.12 (m, 2H), 4.68–4.92 (m, 2H), 5.14 (s, 2H), 6.30 (m, 1H), 7.26–7.35 (m, 10H), 7.86 (s, 3/10H), 8.15 (s, 7/10H); ^{13}C NMR (CDCl_3 , 300 MHz) δ 22.5, 23.4, 26.1, 39.9, 41.8, 43.8, 47.1, 67.5, 128.8, 128.9, 129.0, 129.3, 129.5, 129.8, 134.5, 135.5, 163.5, 170.6, 204.4. HRMS (EI): calcd for $\text{C}_{24}\text{H}_{30}\text{N}_2\text{O}_5$, 426.2155; found 426.2155.

***N*-[(*R*)-2-((*N*-(*O*-Benzyloxy)-*N*-formyl)aminomethyl)-4-methylpentanoyl]-L-alanine benzyl ester (5c).**

(Yield, 71%). $[\alpha]_{\text{D}}^{20} -9.6^\circ$ (c 0.63, CHCl_3); IR (CHCl_3) 1656, 1681, 1743 cm^{-1} ; ^1H NMR (CDCl_3 , 300 MHz) δ 0.86 (d, 6H), 0.96–1.23 (m, 1H), 1.28 (d, 3H), 1.57 (m, 2H), 2.59 (m, 1H), 3.06–3.73 (m, 2H), 4.59 (t, 1H), 4.75–4.98 (m, 2H), 5.15 (q, 2H), 6.16 (m, 1H), 7.267.37 (m, 10H), 7.86 (s, 3/10H), 8.14 (s, 7/10H); ^{13}C NMR (CDCl_3 , 300 MHz) δ 14.6, 18.5, 21.4, 22.5, 23.4, 26.0, 48.4, 60.8, 67.5, 128.6, 128.8, 129.1, 129.5, 129.9, 130.0, 133.9, 135.7, 163.2, 173.6, 204.4. HRMS (EI): calcd for $\text{C}_{25}\text{H}_{32}\text{N}_2\text{O}_5$, 440.2311; found 440.2312.

***N*-[(*R*)-2-((*N*-(*O*-Benzyloxy)-*N*-formyl)aminomethyl)-4-methylpentanoyl]-D-alanine benzyl ester (5d).** (Yield, 72%). $[\alpha]_{\text{D}}^{20} -3.7^\circ$ (c 0.64, CHCl_3); IR (CHCl_3) 1655, 1682, 1743 cm^{-1} ; ^1H NMR (CDCl_3 , 300 MHz) δ 0.86 (d, 6H), 1.12 (m, 1H), 1.36 (d, 3H), 1.56 (m, 2H), 2.61 (m, 1H), 3.68 (m, 2H), 4.56 (m, 1H), 4.73–5.01 (m, 2H), 5.09 (s, 2H), 6.25 (m, 1H), 7.24–7.32 (m, 10H), 7.82 (s, 3/10H), 8.15 (s, 7/10H); ^{13}C NMR (CDCl_3 , 300 MHz) δ 18.8, 22.5, 23.4, 26.2, 39.8, 43.7, 47.3, 48.5, 67.5, 128.6, 128.8, 129.0, 129.1, 129.4, 129.7, 134.6, 135.7, 163.6, 173.5, 204.4. HRMS (EI): calcd for $\text{C}_{25}\text{H}_{32}\text{N}_2\text{O}_5$, 440.2311; found 440.2307.

***N*-[(*R*)-2-((*N*-(*O*-Benzyloxy)-*N*-formyl)aminomethyl)-4-methylpentanoyl]-L-phenylalanine benzyl ester (5e).** (Yield, 78%). $[\alpha]_{\text{D}}^{20} -6.8^\circ$ (c 0.34, CHCl_3); IR (CHCl_3) 1656, 1682, 1742 cm^{-1} ; ^1H NMR (CDCl_3 , 300 MHz) δ 0.80 (d, 6H), 1.21 (m, 1H), 1.50 (m, 2H), 2.53 (m, 1H), 2.93 (m, 2H), 3.66 (m, 2H), 4.67 (t, 1H), 4.88 (s, 2H), 5.08 (q, 2H), 6.06 (m, 1H), 6.96–7.35 (m, 15H), 7.82 (s, 3/10H), 8.09 (s, 7/10H); ^{13}C NMR (CDCl_3 , 300 MHz) δ 22.5, 23.4, 26.0, 38.1, 39.9, 43.9, 46.8, 53.4, 67.6, 127.4, 128.9, 129.0, 129.1, 129.7, 130.1, 135.5, 136.2, 163.3, 171.6, 204.3. HRMS (EI): calcd for $\text{C}_{31}\text{H}_{36}\text{N}_2\text{O}_5$, 516.2624; found 516.2625.

General Procedure for the preparation of 1a–1e. A solution of **5a–5e** in MeOH (20 mL) was stirred for 2 h under hydrogen atmosphere in the presence of 10% Pd-C. The resulting mixture

was filtered and the filtrate was evaporated under reduced pressure to give **1a–1e**. In cases of **1b–1e**, the products were isolated and characterized as salts of dicyclohexylamine.

(*R*)-2-((*N*-formyl-*N*-hydroxy)aminomethyl)-4-methylpentanoic acid amide (1a). (Yield, 90%). $[\alpha]_{\text{D}}^{20} -13.6^\circ$ (c 1.72, MeOH); IR (KBr) 1668, 1689 cm^{-1} ; ^1H NMR (CD_3OD , 300 MHz) δ 0.93 (d, 6H), 1.20 (m, 1H), 1.57 (m, 2H), 2.95 (m, 1H), 3.33–3.75 (m, 2H), 7.85 (s, 7/10H), 8.23 (s, 3/10H); ^{13}C NMR (CD_3OD , 300 MHz) δ 21.4, 22.6, 26.1, 39.1, 42.3, 52.8, 158.5, 163.0, 177.8; HRMS (FAB+) ($\text{M}+\text{H}^+$): calcd for $\text{C}_{15}\text{H}_{24}\text{N}_2\text{O}_3$, 189.1239; found 189.1234.

***N*-[(*R*)-2-((*N*-Formyl-*N*-hydroxy)aminomethyl)-4-methylpentanoyl]glycine (1b).** (Yield, 92%). Mp 153.5–154.5 $^\circ\text{C}$; $[\alpha]_{\text{D}}^{20} -13.3^\circ$ (c 0.12, MeOH); IR (KBr) 1651, 1669, 3389 cm^{-1} ; ^1H NMR (CD_3OD , 300 MHz) δ 0.89 (d, 6H), 1.10–1.36 (m, 11H), 1.55 (m, 2H), 1.67 (d, 2H), 1.81 (m, 4H), 2.03 (m, 4H), 2.61–2.89 (m, 1H), 3.14 (m, 2H), 3.34–3.55 (m, 2H), 3.81–3.86 (m, 1H), 4.04–4.10 (m, 1H), 7.83 (s, 3/10H), 8.25 (s, 7/10H); ^{13}C NMR (CD_3OD , 300 MHz) δ 21.3, 22.6, 24.5, 25.2, 26.1, 29.5, 38.5, 43.7, 50.5, 53.4, 158.5, 163.3, 175.0. Anal. Calcd. for $\text{C}_{22}\text{H}_{41}\text{N}_3\text{O}_5/2\text{H}_2\text{O}$: C, 60.52; H, 9.70; N, 9.62. Found: C, 60.34; H, 9.73; N, 9.63.

***N*-[(*R*)-2-((*N*-Formyl-*N*-hydroxy)aminomethyl)-4-methylpentanoyl]-L-alanine (1c).** (Yield, 88%). Mp 182–183 $^\circ\text{C}$; $[\alpha]_{\text{D}}^{20} -19.2^\circ$ (c 0.59, MeOH); IR (KBr) 1645, 1669, 3341 cm^{-1} ; ^1H NMR (CD_3OD , 300 MHz) δ 0.81–0.88 (m, 6H), 1.09–1.32 (m, 13H), 1.49 (m, 2H), 1.63 (d, 2H), 1.77 (m, 4H), 2.00 (m, 4H), 2.63–2.87 (m, 1H), 3.10 (m, 2H), 3.24–3.51 (m, 1H), 3.61–3.69 (m, 1H), 4.15 (t, 1H), 7.74 (s, 7/10H), 8.19 (s, 3/10H); ^{13}C NMR (CD_3OD , 300 MHz) δ 18.7, 21.7, 22.5, 24.5, 25.2, 26.0, 29.5, 38.7, 43.0, 50.9, 53.4, 158.6, 163.1, 173.5. Anal. calcd for $\text{C}_{23}\text{H}_{43}\text{N}_3\text{O}_5/4\text{H}_2\text{O}$: C, 61.92; H, 9.83; N, 9.42. Found: C, 61.95; H, 10.08; N, 9.44.

***N*-[(*R*)-2-((*N*-Formyl-*N*-hydroxy)aminomethyl)-4-methylpentanoyl]-D-alanine (1d).** (Yield, 90%). Mp 87–89 $^\circ\text{C}$; $[\alpha]_{\text{D}}^{20} -10.5^\circ$ (c 0.65, MeOH); IR (KBr) 1651, 1670, 3388 cm^{-1} ; ^1H NMR (CD_3OD , 300 MHz) δ 0.91 (d, 6H), 1.26 (m, 1H), 1.31–1.34 (m, 15H), 1.56 (m, 2H), 1.82 (m, 4H), 2.05 (m, 4H), 2.70 (m, 1H), 3.13 (m, 2H), 3.42–3.79 (m, 2H), 4.26 (t, 1H), 7.85 (s, 3/10H), 8.26 (s, 7/10H); ^{13}C NMR (CD_3OD , 300 MHz) δ 17.6, 21.4, 22.5, 24.6, 25.2, 26.1, 38.7, 43.5, 50.4, 53.6, 158.7, 163.3, 174.3. Anal. calcd for $\text{C}_{23}\text{H}_{43}\text{N}_3\text{O}_5/3\text{H}_2\text{O}$: C, 61.72; H, 9.83; N, 9.39. Found: C, 61.97; H, 10.09; N, 9.40.

***N*-[(*R*)-2-((*N*-Formyl-*N*-hydroxy)aminomethyl)-4-methylpentanoyl]-L-phenylalanine (1e)** (Yield, 94%). Mp 170–171 $^\circ\text{C}$; $[\alpha]_{\text{D}}^{20} +17.4^\circ$ (c 0.23, MeOH); IR (KBr) 1651, 1668, 3408 cm^{-1} ; ^1H NMR (CD_3OD , 300 MHz) δ 0.74–0.89 (m, 6H), 1.12–1.43 (m, 13H), 1.65 (d, 2H), 1.80 (m, 4H), 1.99 (m, 4H), 2.63–2.85 (m, 1H), 2.96 (m, 1H), 3.07–3.11 (m, 3H), 3.34–3.53 (m, 2H), 4.41 (m, 1H), 7.75 (s, 3/10H), 8.14 (s, 7/10H); ^{13}C NMR (CD_3OD , 300 MHz) δ 21.3, 22.7, 24.5, 25.2, 25.8, 29.5, 38.6, 43.5, 50.5, 53.3, 56.4, 126.3, 128.2, 129.6, 138.7, 158.5, 163.2, 173.9. Anal. calcd for $\text{C}_{29}\text{H}_{47}\text{CN}_3\text{O}_5/3\text{H}_2\text{O}$: C, 66.51; H, 9.17; N, 8.02. Found: C, 66.67; H, 9.10; N, 8.06.

13. Feder, J.; Brougham, L. R.; Wildi, B. S. *Biochemistry* **1974**, *13*, 1186.

14. Matthews, B. W. *Acc. Chem. Res.* **1988**, *21*, 333.

15. Izquierdo, M. C.; Stein, R. L. *J. Am. Chem. Soc.* **1990**, *112*, 6054.

16. Beaumont, A.; O'Donohue, M. J.; Peredes, N.; Rousselet, N.; Assicot, M.; Bohuon, C.; Fourié-Zaluske, M.-C.; Roques, B. *J. Biol. Chem.* **1995**, *270*, 16803.

17. Hangauer, D. G.; Monzingo, A. F.; Matthews, B. W. *Biochemistry* **1984**, *23*, 5730.

18. (a) Antonczak, S.; Monard, G.; Ruiz-Lopez, M. F.; Revail, J.-L. *J. Am. Chem. Soc.* **1998**, *120*, 8825. (b) Antonczak, S.; Monard, G.; Ruiz-Lopez, M. F.; Revail, J.-L. *J. Mol. Model* **2000**, *6*, 527. (c) Pelmeshnikov, V.; Blomberg, M. R. A.; Siegbahn, P. E. M. *J. Biol. Inorg. Chem.* **2002**, *7*, 284.

19. Kim, S.-J.; Kim, D. H.; Park, J. D.; Woo, J.-R.; Jin, Y.; Ryu, S. E. *Bioorg. Med. Chem.* **2003**, *11*, 2421.
20. (a) The deprotonation may most likely be resulted as a consequence of the high Lewis acidity of the zinc ion: Izquierdo-Martin, M.; Stein, R. L. *J. Am. Chem. Soc.* **1992**, *114*, 325. (b) Cross, J. B.; Duca, J. S.; Kaminski, J. J.; Madison, V. S. *J. Am. Chem. Soc.* **2002**, *124*, 11004.
21. Morihara, K.; Tsuzuki, H. *Eur. J. Biochem.* **1970**, *15*, 374.